

# Interference between Dipolar and Quadrupolar Interactions in the Slow Tumbling Limit: A Source of Line Shift and Relaxation in $^2\text{H}$ -Labeled Compounds

Stephan Grzesiek\* and Ad Bax

Contribution from the Laboratory of Chemical Physics, National Institute of Diabetes and Digestive and Kidney Diseases, National Institutes of Health, Bethesda, Maryland 20892

Received June 23, 1994\*

**Abstract:** Using Redfield's theory of relaxation, it is demonstrated that interference of the dipolar and quadrupolar interactions between a spin- $1/2$  and a spin-1 nucleus causes a frequency shift of the spin- $1/2$  transition coupled to the  $m = 0$  state of the spin-1 nucleus relative to the transitions coupled to the  $m = \pm 1$  states. This frequency shift depends on the rotational correlation time: it vanishes in the fast tumbling limit and reaches a constant in the slow motion limit which coincides with the results for static powder samples. For a  $^{13}\text{C}$  nucleus which is  $J$ -coupled to a directly bonded  $^2\text{H}$ , this results in an asymmetric triplet pattern for molecular motions slower than at the  $T_1$  minimum of the spin-1 nucleus. The center component of the triplet is shifted downfield by an amount which depends inversely on the static magnetic field strength. Although rapid longitudinal relaxation of the spin-1 nucleus collapses both the  $J$  multiplet and the interference-induced splitting, the interference contribution to the line width of the spin- $1/2$  nucleus can only be removed in part by high-power decoupling of the spin-1 nucleus. Experimental results are demonstrated for the  $^{13}\text{C}$  spectrum of perdeuterated glycerol, where the rotational correlation time is varied with temperature. Application of the theory to other nuclei indicates that dipolar/quadrupolar interference also results in additional line broadening for proteins in solution that are enriched in  $^2\text{H}$ , and for amide protons attached to  $^{14}\text{N}$ .

## Introduction

Substitution of  $^1\text{H}$  by  $^2\text{H}$  in solution NMR studies of proteins has been proposed<sup>1–11</sup> to alleviate the problems of  $^1\text{H}$  resonance overlap and of strong dipolar relaxation caused by the high gyromagnetic ratio of protons. Two- to threefold line narrowing of  $^{13}\text{C}_\alpha$  resonances bound to  $^2\text{H}$  has also been observed experimentally for the proteins calcineurin B<sup>10</sup> and thioredoxin<sup>11</sup> as compared to protonated  $\alpha$ -carbons. The  $^2\text{H}$ -coupled  $^{13}\text{C}$  multiplets shown for thioredoxin exhibit a curious asymmetry,<sup>11</sup> but no explanation for this unusual multiplet shape has been reported. We show that the asymmetry of the  $^{13}\text{C}$  line can readily be observed in pure deuterated glycerol at natural abundance of  $^{13}\text{C}$  where the correlation time can be varied over many orders of magnitude by changing the temperature. As described below, this asymmetry is caused by interference, also referred to as cross correlation, between the dipolar and quadrupolar interactions. Interference effects between dipolar and CSA and dipolar and quadrupolar interactions as well as between dipolar and dipolar interactions have been described in the literature<sup>12–25</sup> mainly as a mechanism

of differential line broadening which is due to the real part of the spectral density. The asymmetry of the  $^{13}\text{C}$  triplet, however, is caused by the imaginary component of the spectral density in a way similar to the dynamic frequency shift observed for the quadrupolar nuclei as discussed by Werbelow.<sup>26</sup> In the slow motion limit, the asymmetric splitting reaches a constant which is identical to expressions found for powder patterns in the high-field limit of the  $^{13}\text{C}$ - $^{14}\text{N}$  dipolar/quadrupolar Hamiltonian in CP/MAS spectroscopy.<sup>27–29</sup> The asymmetric splitting in the multiplet of a spin- $1/2$  nucleus coupled to a spin-1 nucleus together with the spin flips of the spin-1 nucleus acts as a line-broadening mechanism in liquids. However, in contrast to scalar relaxation of the second kind,<sup>30</sup> this line broadening can only in part be suppressed by high-power deuterium decoupling.

## Experimental Section

Glycerol, uniformly (98%) enriched in  $^2\text{H}$  (glycerol- $d_8$ , Cambridge Isotope Laboratories) was distilled once under vacuum and rapidly transferred into NMR sample tubes under an argon atmosphere. The sample tubes were then closed with a cap and sealed with Teflon tape.

\* Abstract published in *Advance ACS Abstracts*, October 1, 1994.

(1) Crespi, H. L.; Rosenberg, R. M.; Katz, J. J. *Science* **1968**, *161*, 795–798.

(2) Markley, J. L.; Putter, I.; Jardetzky, O. *Science* **1968**, *161*, 1249–1251.

(3) Browne, D. T.; Kenyon, G. L.; Packer, E. L.; Sternlicht, H.; Wilson, D. M. *J. Am. Chem. Soc.* **1973**, *95*, 1316–1323.

(4) Chan, T. M.; Markley, J. L. *J. Am. Chem. Soc.* **1982**, *104*, 4010–4011.

(5) Griffey, R. H.; Redfield, A. G.; Loomis, R. E.; Dahlquist, F. W. *Biochemistry* **1985**, *24*, 817–822.

(6) LeMaster, D. M.; Richards, F. M. *Biochemistry* **1985**, *24*, 7263–7268.

(7) McIntosh, L. P.; Griffey, R. H.; Muchmore, D. C.; Nielson, C. P.; Redfield, A. G.; Dahlquist, F. W. *Proc. Natl. Acad. Sci. U.S.A.* **1987**, *84*, 1244–1248.

(8) LeMaster, D. M.; Richards, F. M. *Biochemistry* **1988**, *27*, 142–150.

(9) Arrowsmith, C. H.; Pachter, R.; Altman, R. B.; Iyer, S. B.; Jardetzky, O. *Biochemistry* **1990**, *29*, 6332–6341.

(10) Grzesiek, S.; Anglister, J.; Ren, H.; Bax, A. *J. Am. Chem. Soc.* **1993**, *115*, 4369–4370.

(11) Kushlan, D. M.; LeMaster, D. M. *J. Biomol. NMR* **1993**, *3*, 701–708.

(12) Blicharski, J. S. *Phys. Lett. A* **1967**, *24*, 608–610.

(13) Blicharski, J. S. *Acta Phys. Pol.* **1969**, *36*, 211–218.

(14) Deleted in proof.

(15) Deleted in proof.

(16) Deleted in proof.

(17) Blicharski, J. S.; Nosel, W. *Acta Phys. Pol.*, **A** **1972**, *42*, 223–232.

(18) Werbelow, L. G.; Grant, D. M. In *Advances in Magnetic Resonance*; Waugh, J. S., Ed.; Academic Press: San Diego, 1977; Vol. 9, p 189.

(19) Vold, R. L.; Vold, R. R. *Prog. NMR Spectrosc.* **1978**, *12*, 79–133.

(20) Gueron, M.; Leroy, J. L.; Griffey, R. H. *J. Am. Chem. Soc.* **1983**, *105*, 7262–7266.

(21) Goldman, M. *J. Magn. Reson.* **1984**, *60*, 437–452.

(22) Wimperis, S.; Bodenhausen, G. *Mol. Phys.* **1989**, *66*, 897–919.

(23) Dalvit, C. J. *J. Magn. Reson.* **1991**, *95*, 410–416.

(24) Bull, T. E. *Prog. NMR Spectrosc.* **1992**, *24*, 377–410.

(25) Kay, L. E.; Nicholson, L. K.; Delaglio, F.; Bax, A.; Torchia, D. A. *J. Magn. Reson.* **1992**, *97*, 359–375.

(26) Werbelow, L. G. *J. Chem. Phys.* **1979**, *70*, 5381–5383.

(27) Hexem, J. G.; Frey, M. H.; Opella, S. J. *J. Chem. Phys.* **1982**, *77*, 3847–3856.

(28) Olivieri, A. C.; Frydman, L.; Djaz, L. E. *J. Magn. Reson.* **1987**, *75*, 50–62.

(29) Eichele, K.; Lumsden, M. D.; Wasylishen, R. E. *J. Phys. Chem.* **1993**, *97*, 8909–8916.

(30) Abragam, A. *The Principles of Nuclear Magnetism*; Clarendon Press: Oxford, 1961; p 309.

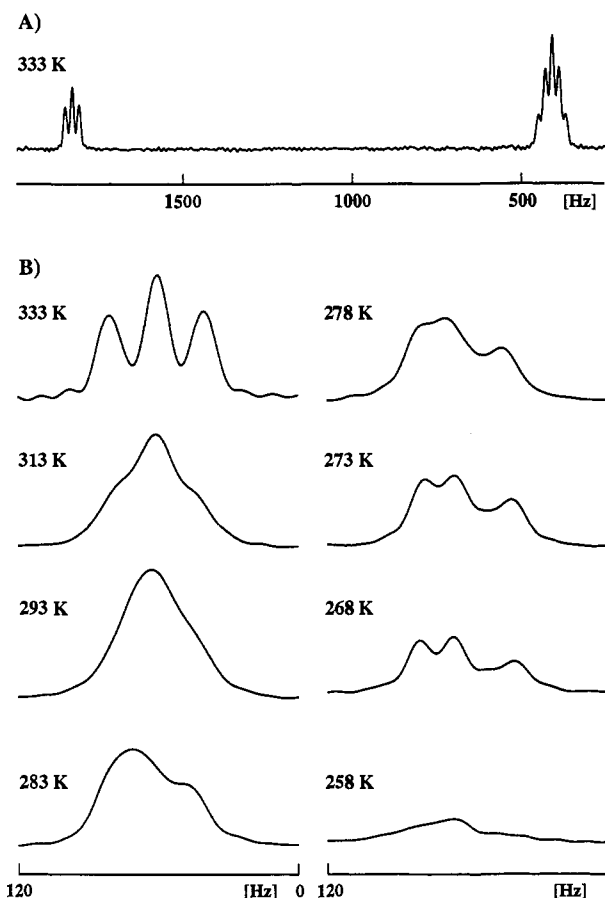


**Figure 1.**  $^{13}\text{C}$  natural abundance spectrum of glycerol- $d_8$  at various temperatures at a magnetic field strength of 600 MHz proton Larmor frequency: (A) complete spectrum at 333 K, (B) spectral region of the methine triplet in the temperature range from 333 to 258 K. Spectra were recorded with the spectrometer in the unlocked mode; therefore, the frequency reference is arbitrary. A total of 32 transients were recorded per spectrum.

No change in  $^1\text{H}$  and  $^{13}\text{C}$  spectra or relaxation times was observed on these samples over a period of 6 months. NMR experiments were carried out either on a Bruker AMX600 three-channel spectrometer or on a Bruker AMX360 two-channel spectrometer. For the numerical line shape simulations the software system Mathematica (Wolfram Research Inc.) was used.

## Results

**Asymmetric  $^{13}\text{C}$ - $^2\text{H}$  Triplet.** Figure 1A depicts the natural abundance  $^{13}\text{C}$  spectrum of glycerol- $d_8$  at 333 K and at a magnetic field strength of 600 MHz proton Larmor frequency. Clearly visible is the downfield-shifted symmetric triplet of the central methine carbon. It corresponds to a 20 Hz scalar coupling of the central spin-1 deuterium to the  $^{13}\text{C}$  methine carbon. The two equivalent methylene carbons, each attached to two equivalent deuterons, give rise to the symmetric pentuplet in the upfield part of the spectrum. As the temperature is lowered from 333 to 258 K (Figure 1B), the resonance lines become broader until the methine triplet collapses into a singlet at the  $T_1$  minimum of deuterium, at about 293 K. At even lower temperatures the lines become narrower again, and a triplet can be observed between 278 and 268 K. At 258 K, the outer lines of the triplet have nearly broadened beyond detection. A surprising feature of the triplet below 293 K is its distinct asymmetry, which at 268 K amounts to a low-field shift of about 5.2 Hz of the center line with respect to the center of the outer lines (Figure 2A). At a magnetic field strength of 360 MHz proton Larmor frequency, the triplet at 268 K is less well resolved, due to the shorter  $^2\text{H}$   $T_1$  value. However, a strongly resolution enhanced spectrum

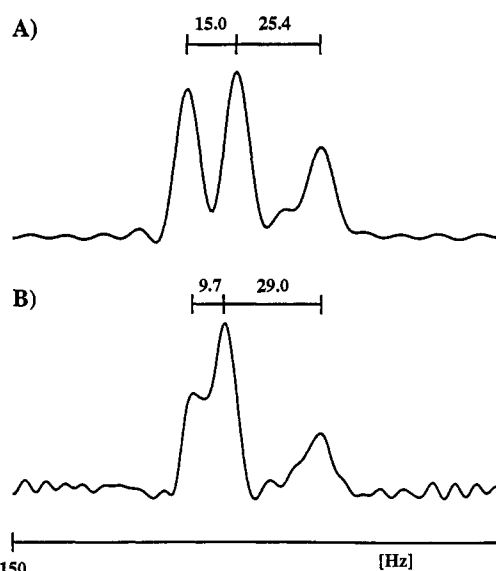


**Figure 2.**  $^{13}\text{C}$  natural abundance spectrum of the methine triplet of glycerol- $d_8$  at 268 K: (A) magnetic field strength of 600 MHz proton Larmor frequency, 2600 averaged transients, (B) magnetic field strength of 360 MHz proton Larmor frequency, 3072 averaged transients. Digital resolution enhancement was used to resolve the individual components of the triplet.

(Figure 2B) shows that the asymmetric shift of the center line increases to ca. 9 Hz, indicating that the effect is inversely proportional to the strength of the static magnetic field.

**Redfield Theory of the Dipolar/Quadrupolar Interference.** As described below, the asymmetry of the triplet follows in a straightforward manner from Redfield theory.<sup>31</sup> The spin system can be described by the following Hamiltonian:<sup>32</sup>

$$\hbar\mathcal{H} = \hbar\mathcal{H}_S + \hbar\mathcal{H}_{SL}(t) \quad (1)$$

where  $\mathcal{H}_S$  is the spin Hamiltonian and  $\mathcal{H}_{SL}(t)$  the Hamiltonian of the spin-lattice coupling in the interaction picture. Assuming cylindrical symmetry for the quadrupolar interaction (asymmetry parameter  $\eta = 0$ ), both quadrupolar and dipolar spin-lattice interactions can be expressed in the following form:

$$\mathcal{H}(t, \Omega) = \sum_{m=-2}^2 \sum_{\alpha} G X_m^{\alpha} Y_{2-m}(\Omega) (-1)^m \exp(i\omega_m^{\alpha} t) \quad (2)$$

where  $G$  is a coupling constant,  $X_m^{\alpha}$  the spin-dependent part of the interaction,  $Y_{2m}$  a second-order spherical harmonic at the Euler angles  $\Omega = (\theta, \phi)$  representing the orientation with respect to the external magnetic field of either the internuclear vector in the dipolar case or the principal axis of the quadrupolar tensor. The characteristic frequency associated with the interaction representation of spin operator  $X_m^{\alpha}$  is given by  $\omega_m^{\alpha}$ . Denoting dipolar and quadrupolar terms by superscripts D and Q, the coupling constants  $G$ , spin operators  $X_m^{\alpha}$ , and transition frequencies  $\omega_m^{\alpha}$  take the following form:

$${}^D G = -\left(\frac{24\pi}{5}\right)^{1/2} \frac{\gamma_I \gamma_S \hbar}{r^3} \quad (3a)$$

$${}^Q G = \left(\frac{4\pi}{5}\right)^{1/2} \frac{e^2 q Q}{4\hbar} \quad (3b)$$

(31) Redfield, A. G. *Adv. Magn. Reson.* **1965**, *1*, 1-32.

(32) Goldman, M. *Quantum Description of High-Resolution NMR in Liquids*; Clarendon Press: Oxford, 1988; p 236 ff.

$${}^D X_0^1 = (2/\sqrt{6}) I_z S_z, \quad {}^D \omega_0^1 = 0 \quad (4a)$$

$${}^D X_0^2 = -(1/2\sqrt{6}) I_- S_+, \quad {}^D \omega_0^2 = \omega_S - \omega_I$$

$${}^D X_0^3 = -(1/2\sqrt{6}) I_+ S_-, \quad {}^D \omega_0^3 = \omega_I - \omega_S$$

$${}^D X_1^1 = -(1/2) I_z S_+, \quad {}^D \omega_1^1 = \omega_S$$

$${}^D X_1^2 = -(1/2) I_+ S_z, \quad {}^D \omega_1^2 = \omega_I$$

$${}^D X_2^1 = (1/2) I_+ S_+, \quad {}^D \omega_2^1 = \omega_I + \omega_S$$

$${}^Q X_0^1 = 2S_z^2 - (1/2)(S_+ S_- + S_- S_+), \quad {}^Q \omega_0^1 = 0 \quad (4b)$$

$${}^Q X_1^1 = -(3/2)^{1/2} (S_z S_+ + S_+ S_z), \quad {}^Q \omega_1^1 = \omega_S$$

$${}^Q X_2^1 = (3/2)^{1/2} S_+^2, \quad {}^Q \omega_2^1 = 2\omega_S$$

$$X_m^{\alpha\prime} = (-1)^m X_{-m}^\alpha, \quad \omega_m^\alpha = -\omega_{-m}^\alpha \text{ for } m \neq 0 \quad (4c)$$

where  $I$  and  $S$  denote the spin- $1/2$  and spin-1 nuclei as well as their spin operators, respectively,  $r$  is the internuclear distance,  $eQ$  the nuclear quadrupole moment, and  $eq$  the electrical field gradient, and  $X^\dagger$  denotes the Hermitian adjoint of the operator  $X$ . Under a number of common assumptions, detailed by Abragam,<sup>33</sup> the Liouville equation of motion for the density matrix  $\sigma$  in the interaction representation is commonly written as

$$\frac{d\sigma}{dt} = (-i\mathcal{H}_S - (1/4\pi) \sum_{m=-2}^2 \sum_{\alpha, \alpha', I, I'} I^{\alpha'} G^I X_m^{\alpha'} X_m^{\alpha\dagger} P_2(\cos \theta_{II'}) \times J(\omega_m^\alpha, \tau)) \sigma \quad (5)$$

where the  $X$  is the commutator superoperator<sup>34</sup> of the operator  $X$  and the second sum is to be taken over all possible values ( $\alpha, \alpha', I, I'$ ) for which  $\omega_m^\alpha = \omega_m^{\alpha'}$  (secular approximation).  $P_2$  is the second-order Legendre polynomial and  $\theta_{II'}$  is the angle between the two principal vectors (internuclear vector or principal axis of the quadrupolar tensor) of the two interactions  $I$  and  $I'$  involved.<sup>21</sup> The function  $J(\omega, \tau)$  is the complex spectral density at frequency  $\omega$  and (isotropic) rotational correlation time  $\tau$ :

$$J(\omega, \tau) = \frac{1}{1/\tau - i\omega} = \frac{\tau}{1 + \omega^2 \tau^2} + i \frac{\omega \tau^2}{1 + \omega^2 \tau^2} \quad (6)$$

where the imaginary part which is usually neglected has been retained. When calculating the evolution of the transverse spin- $1/2$  magnetization  $I_+$  under scalar coupling to the deuteron ( $\mathcal{H}_S = 2\pi J_{IS} I_z S_z$ ) including the effects of dipolar and quadrupolar relaxation, it is seen that due to the secular approximation only the following three density matrix states become intermixed by the Liouville equation (eq 5):

$$||+1\rangle\rangle = (1/2) I_+ (S_z^2 + S_z) \quad (7)$$

$$||0\rangle\rangle = I_+ (1 - S_z^2)$$

$$||-1\rangle\rangle = (1/2) I_+ (S_z^2 - S_z)$$

where the bra- and -ket notation for density matrix states of Sanctuary<sup>35</sup> has been used.

(33) Reference 30, p 276.

(34) Ernst, R. R.; Bodenhausen, G.; Wokaun, A. *Principles of Nuclear Magnetic Resonance in One and Two Dimensions*; Clarendon Press: Oxford, 1987.

(35) Sanctuary, B. C.; Selwyn, L. *J. Chem. Phys.* **1981**, *74*, 906-912.

Although tedious, calculation of the matrix elements is straightforward. In eq 5 the products  $\frac{{}^D X_m^\alpha, {}^D X_m^{\alpha\dagger}}$  describe pure dipolar relaxation and the products  $\frac{{}^Q X_m^\alpha, {}^Q X_m^{\alpha\dagger}}$  describe pure quadrupolar relaxation. Their relevant matrix elements are given in the Appendix. Besides those conventional sources of relaxation, the following dipolar/quadrupolar interference terms are also allowed by the secular approximation in eq 5:

$$\langle\langle i | \frac{{}^D X_0^1, {}^Q X_0^1}{r^3} | j \rangle\rangle = \langle\langle i | \frac{{}^Q X_0^1, {}^D X_0^1}{r^3} | j \rangle\rangle = 0 \quad (8)$$

$$\langle\langle i | \frac{{}^D X_1^1, {}^Q X_1^1}{r^3} + \frac{{}^Q X_1^1, {}^D X_1^1}{r^3} | j \rangle\rangle =$$

$$-\langle\langle i | \frac{{}^D X_{-1}^1, {}^Q X_{-1}^1}{r^3} + \frac{{}^Q X_{-1}^1, {}^D X_{-1}^1}{r^3} | j \rangle\rangle = \left(\frac{3}{2}\right)^{1/2} \begin{pmatrix} 1 & 0 & 0 \\ 0 & -2 & 0 \\ 0 & 0 & 1 \end{pmatrix}$$

with  $i, j \in \{1, 0, -1\}$ .

The frequencies  ${}^D \omega_1^1 = {}^Q \omega_1^1$  and  ${}^D \omega_{-1}^1 = {}^Q \omega_{-1}^1$  associated with the nonvanishing matrix elements of eq 8 are just the Larmor frequencies  $\pm\omega_S$  of the deuteron. Since the real and imaginary parts of the spectral density function are even and odd functions in  $\omega$ , summation over  $m = +1$  and  $m = -1$  of those interference terms in eq 5 leaves only the imaginary component intact. Therefore, the dipolar/quadrupolar interference terms lead to an energy shift of the different components of the spin- $1/2$  transverse triplet (eq 7). From eq 8, it is clear that the shift is in opposite directions for the central ( $||0\rangle\rangle$ ) and outer ( $||\pm 1\rangle\rangle$ ) components, leading to a net shift  $\Delta$  of the center component with respect to the center of the two outer components, given by

$$\Delta = \frac{9}{20\pi} \frac{\gamma_I \gamma_S \hbar}{r^3} \frac{e^2 q Q}{\hbar} P_2(\cos \theta_{DQ}) \frac{\omega \tau^2}{1 + \omega^2 \tau^2} \quad (9)$$

From eq 9 it is seen that the effect vanishes in the extreme narrowing limit ( $\omega \tau \ll 1$ ). For the slow motion limit ( $\omega \tau \gg 1$ ), it is inversely proportional to the magnetic field strength, as expected from Figure 2.

In high-resolution solid-state NMR spectra of spin- $1/2$  nuclei adjacent to quadrupolar nuclei, characteristic asymmetric line shapes are well known and have been explained by the deviations from the Zeeman states of the quadrupolar nucleus wave functions due to the strong quadrupolar field.<sup>27-29,36-43</sup> These perturbed wave functions of the quadrupolar nucleus in turn couple back to the spin- $1/2$  states by the dipolar interaction. As a result, e.g., in a  $^{13}\text{C}$ - $^{14}\text{N}$  system, the components of the  $^{13}\text{C}$  line coupled to the  $^{14}\text{N}$   $m = 0$  and  $m = \pm 1$  spin states shift in opposite directions and give rise to the asymmetric line shape. The physical mechanism responsible for this phenomenon is exactly the same. It is therefore not surprising that the slow motion limit of eq 9, i.e.,  $\omega \tau^2 / (1 + \omega^2 \tau^2) \rightarrow 1/\omega$ , coincides with equations found for this asymmetric splitting in solid-state NMR for powder pattern samples of spin- $1/2$ -spin-1 systems in the high-field approximation, provided that this approximation is carried out to the same order.<sup>27-29</sup> Indeed, the first-order perturbation of the  $^{14}\text{N}$  wave functions that was used to calculate the energy shift due to the dipolar interaction<sup>27-29</sup> amounts to a second-order perturbation

(36) VanderHart, D. L.; Gutowski, H. S.; Farrar, T. C. *J. Am. Chem. Soc.* **1967**, *89*, 5056-5057.

(37) Spiess, H. W. *NMR. Basic Principles and Progress*; Springer-Verlag: Berlin, 1978; Vol. 15, pp 55-214.

(38) Hexem, J. G.; Frey, M. H.; Opella, S. J. *J. Am. Chem. Soc.* **1981**, *103*, 224-226.

(39) Naito, A.; Ganapathy, S.; McDowell, C. A. *J. Chem. Phys.* **1981**, *74*, 5393-5397.

(40) Zumbulyadis, N.; Henrichs, P. M.; Young, R. H. *J. Chem. Phys.* **1981**, *75*, 1603-1611.

(41) Naito, A.; Ganapathy, S.; McDowell, C. A. *J. Magn. Reson.* **1982**, *48*, 367-381.

(42) Ripmeester, J. A.; Tse, J. S.; Davidson, D. W. *Chem. Phys. Lett.* **1982**, *86*, 428-433.

(43) Gan, Z.; Grant, D. M. *J. Magn. Reson.* **1990**, *90*, 522-534.

for the energy. Regarding the energy shifts of the transitions, this is equivalent to the second-order time-dependent perturbation treatment underlying the Redfield approximation. In a more pictorial representation, one could say that because of the large quadrupolar coupling the axis of quantization of the quadrupolar nucleus deviates from the direction of the Zeeman field. In Redfield's theory (where the quadrupolar coupling is still assumed to be small compared to the Zeeman splitting) the correlation time dependence of eq 9 defines the point at which the molecular motion becomes slow enough such that this tilt of the axis of quantization becomes noticeable as a line shift of the spin- $1/2$  nucleus.

For the methine carbon of glycerol with a carbon-deuteron distance of 1.09 Å, a quadrupolar coupling constant  $e^2qQ/h$  of 170 kHz,<sup>44,45</sup>  $\eta = 0$ , and the main axis of the quadrupolar tensor and the internuclear vector collinear ( $\theta_{DQ} = 0$ ), eq 9 indicates that the shift of the center line  $\Delta$  becomes 5.9 Hz in the slow motion limit at a magnetic field strength of 600 MHz proton Larmor frequency. This is in good agreement with the value of 5.2 Hz observed in Figure 2, considering that the effect of the mixing of the lines due to the deuterium spin flips has not been taken into account.

Equation 5 in the three-dimensional invariant subspace defined by eq 7 can be solved in a closed, but very lengthy, analytical form. However, no immediate insight is gained from this solution. Instead we choose to integrate eq 5 numerically using the software system Mathematica. In eq 5, the one-bond deuterium-carbon  $J$  coupling is accounted for by setting  $\mathcal{H}_S = 2\pi J_{IS}I_zS_z$ . A value of 20 Hz was used for the coupling constant  $J_{IS}$ . For the relaxation terms, the same parameter values as above were chosen: a magnetic field strength of 600 MHz proton Larmor frequency, a carbon-deuteron distance of 1.09 Å, a quadrupolar coupling constant of 170 kHz,  $\eta = 0$ , and  $\theta_{DQ} = 0$ . Figure 3 shows the Fourier-transformed frequency domain solutions of eq 5 for the transverse magnetization  $I_+$  for values of the correlation time  $\tau$ , ranging from extreme narrowing at 10 ps to extreme slow motion at 500 ns. Figure 3 completely reproduces the experimental behavior of the triplet in Figure 1, i.e., the symmetry at fast correlation times, the coalescence of the triplet into a singlet at the  $T_1$  minimum at a  $\tau$  of about 1–3 ns, the appearance of the asymmetry for correlation times longer than at the  $T_1$  minimum, and the final disappearance of the outer components at very long correlation times.

For a more quantitative comparison, an estimate of the experimental correlation times is required. As the deuterium relaxation is completely dominated by the quadrupolar interaction, an estimate of the rotational correlation time can be calculated from the deuterium  $T_1$  and  $T_2$  values.<sup>46</sup> This determination is however complicated by the fact that the deuterium lines for the methine and methylene groups become indistinguishable at temperatures below 283 K at 600 MHz proton frequency. Since the  $^2\text{H}$   $T_1$  and  $T_2$  values for the methylene group are about 30–40% larger than for the methine group in the resolved case ( $T > 283$  K), averaging of the relaxation times at the lower temperatures may introduce a substantial error. Nevertheless, an average of the correlation times determined from the deuterium  $T_1$  and  $T_2$  values for a quadrupolar coupling constant of 170 kHz is listed in Table 1. Clearly, within experimental error, the measured correlation times and line shapes correspond very well to the theoretical line shapes and correlation times of Figure 3.

**Effect of Strong Deuterium Decoupling Fields.** Abragam<sup>47</sup> has shown that the Redfield matrix, i.e., the double sum in eq 5, stays invariant, when time-dependent perturbations, such as radio-frequency (RF) fields, are added to the Hamiltonian of eq 1, as

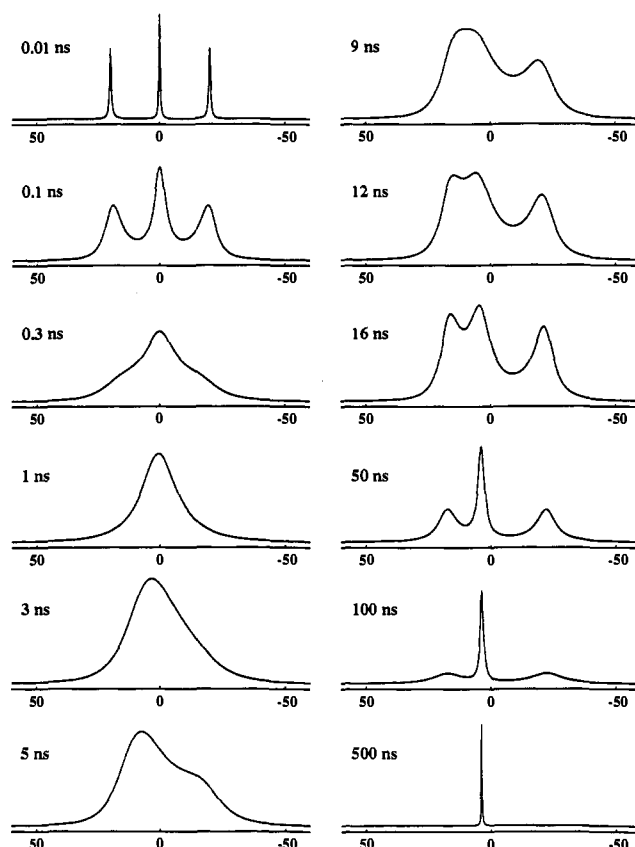


**Figure 3.** Numerical simulations of the methine  $^{13}\text{C}$ - $^2\text{H}$  triplet at isotropic rotational correlation times ranging from 10 ps to 500 ns. Spectra were calculated as the Fourier transforms of the numerical solutions of eq 5 for a total length of the FID of 25 s and a field strength of 14 T (600 MHz  $^1\text{H}$  Larmor frequency). Frequencies are given in hertz.

**Table 1.** Rotational Correlation Times,  $\tau$ , of the Glycerol Methine Deuteron<sup>a</sup>

$T/\text{K}$	$\tau/\text{ns}$	$T/\text{K}$	$\tau/\text{ns}$
333	$0.11 \pm 0.01$	278	$6.3 \pm 1.8$
313	$0.35 \pm 0.01$	273	$9.7 \pm 3.4$
293	$1.4 \pm 0.3$	268	$17 \pm 10$
283	$3.7 \pm 1.2$	258	nd <sup>b</sup>

<sup>a</sup> As determined by the  $^2\text{H}$   $T_1$  and  $T_2$  values (see text). <sup>b</sup> No values could be determined as  $T_2$  was already on the order of the pulse lengths ( $\sim 100$   $\mu\text{s}$ ).

long as the strength of the perturbation is small compared to the inverse of the rotational correlation time. Achievable RF field strengths on commercial spectrometers are well below  $\tau^{-1}$  for liquids. Therefore, the effect of a decoupling field can be included in the Liouville equation (eq 5), by simply adding the decoupling field term to the spin Hamiltonian  $\mathcal{H}_S$ . For a decoupling field of strength  $\omega_1$  applied along the  $x$ -axis at the resonance frequency of the deuterium, this field term is written as  $\omega_1 S_x$ , where counterrotating terms have been neglected. For field strengths much larger than the scalar coupling constant  $J_{IS}$ , the effect of the scalar coupling and the scalar relaxation of the second kind vanishes for the transverse evolution of spin  $I$ .<sup>48</sup> It is not immediately obvious what happens to the asymmetric splitting in the case of dipolar/quadrupolar interference. Inclusion of  $\omega_1 S_x$  in  $\mathcal{H}_S$  has the effect that the  $I_+$  term no longer only evolves in the three-dimensional subspace of eq 7, since the decoupling field together with the Redfield matrix intermixes all density matrix states of the deuterium. The subspace for the evolution of  $I_+$  therefore becomes nine-dimensional.

We briefly discuss results of a numerical solution for the case of the carbon-deuteron spin system at a rotational correlation

(44) Derbyshire, W.; Gorvin, T. C.; Warner, D. *Mol. Phys.* **1969**, *17*, 401–407.

(45) Burnett, L. J.; Muller, B. H. *J. Chem. Phys.* **1971**, *55*, 5829–5831.

(46) Reference 30, p 314.

(47) Reference 30, p 516.

(48) Reference 30, p 538.

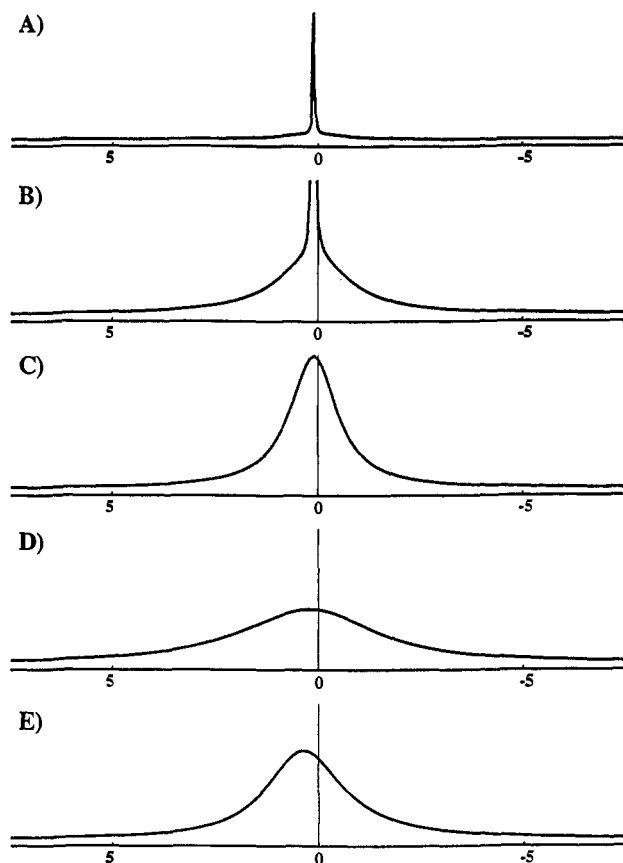


**Figure 4.** Numerical simulations as in Figure 3 of the methine  $^{13}\text{C}$ - $^2\text{H}$  triplet without the scalar coupling term for a 16 ns rotational correlation time. The horizontal scale is hertz. (A) Only relaxation due to the  $^{13}\text{C}$ - $^2\text{H}$  dipolar interaction is considered. (B) is the same as (A) at a 10 times larger vertical scale. (C) to (E) are at the same vertical scale as (B). (C) is the same as (B), but also effects of the pure quadrupole relaxation of the  $^2\text{H}$  nucleus are included. (D) is the same as (C), but in addition the dipolar/quadrupolar cross term with  $\theta_{\text{DQ}} = 0$  is included. (E) is the same as (D), but in addition a 2 kHz RF field is applied along the  $x$ -axis for the  $^2\text{H}$  nuclei.

time of 16 ns (Figure 4). For the sake of simplicity, the  $J$ -coupling term which is suppressed by the decoupling field has not been included in the calculations. Figure 4A (Figure 4B 10 $\times$  larger scale) shows the line shape of the carbon spin relaxed only by dipolar coupling (1.09 Å) to the deuteron (i.e., quadrupolar/dipolar interference and quadrupolar relaxation have not been included in the simulation): a slightly downfield shifted ( $\sim 0.1$  Hz), very narrow ( $< 0.1$  Hz) line sits on the background of a broad ( $\sim 2$  Hz) line. Explanation of this line shape follows immediately from the dipolar terms in the Liouville equation. The rotational correlation time of 16 ns is well in the slow tumbling regime. Therefore, the real part of the spectral density is only significant for zero frequencies, i.e., only  $J(\omega_0^1, \tau) = \tau$  contributes significantly to the line shape. Inspection of the matrix  $\langle \langle i | \rho X_0^1 \cdot X_0^1 | j \rangle \rangle$  (Appendix) shows that the Redfield matrix is diagonal for this spectral density with a vanishing decay for the central line and a decay constant of  $(4/5)((\gamma_I \gamma_S \hbar)^2 / r^6) \tau$  for the outer lines, leading to a line width of 2.1 Hz. The imaginary parts of the spectral density do not cancel in the summation of eq 5, and they account for the slight shift of both the central and outer lines to higher frequencies.

When the quadrupolar relaxation (without the dipolar/quadrupolar cross term) is included in the calculations (Figure 4C), the rapid deuteron spin flips average the narrow central line and the broad outer lines, and one broad line of 1.4 Hz width appears. Note that this situation is also realized in eq 5 with the dipolar/quadrupolar cross term included, if the dipolar and quadrupolar vectors are at the magic angle with respect to each

other ( $P_2(\cos \theta_{\text{DQ}}) = 0$ ). Taking into account the dipolar/quadrupolar interference effect with both dipolar and quadrupolar vectors parallel (Figure 4D) broadens the line to  $\sim 4$  Hz, since the outer and central lines are now split by 5.9 Hz as discussed above. Decoupling the deuteron with a 2 kHz decoupling field (Figure 4E) narrows the line again to about 2.3 Hz. However, the line width of 1.4 Hz without the interference effect is not reached. An increase in the decoupling field strength to 20 kHz does not change the appearance of the spectrum any further (not shown).

**Dipolar/Quadrupolar Splitting for Other Spin- $1/2$ -Spin-1 Systems.** The theory outlined above applies to all spin- $1/2$ -spin-1 systems. In the slow motion limit for a proton separated by 2 Å from a deuteron,  $\theta_{\text{DQ}} = 0$ , and  $\eta = 0$ , at a proton Larmor frequency of 600 MHz, the triplet splitting  $\Delta$  is 3.8 Hz (eq 9). In a macromolecule, this situation however is rarely realized, since the bond vector of nearby deuterons which essentially determines the direction of the quadrupolar tensor is rarely aligned parallel to the internuclear distance vector. Therefore, the term  $P_2(\cos \theta_{\text{DQ}})$  is usually smaller than 1 for neighboring proton-deuteron pairs. For example, in the common case of a tetrahedral  $\text{C}^1\text{H}^2\text{H}$  group,  $\theta_{\text{DQ}}$  is about  $35^\circ$  and the proton-deuteron distance is about 1.8 Å. This leads to a triplet splitting of 2.6 Hz. From the matrix elements of  $\langle \langle i | \rho X_1^1 \cdot Q X_1^1 | j \rangle \rangle$  (Appendix) the quadrupolar spin flip rate  $k$  between the  $|0\rangle$  and  $|\pm 1\rangle$  states, i.e., the center and outer components of the proton line, is calculated as

$$k = \frac{3\sqrt{2}}{40} \left( \frac{e^2 q Q}{\hbar} \right)^2 \frac{\tau}{1 + \omega_S^2 \tau^2} \quad (10)$$

For the deuteron ( $\chi = 170$  kHz,  $\eta = 0$ ) at 8 ns (16 ns) rotational correlation time, this flip rate is 43 Hz (22 Hz). Therefore, the exchange between the outer and center components of the  $^1\text{H}$  triplet is in the fast limit. With the assumption of a fast exchange in the slow motion limit ( $\omega_S \tau \gg 1$ ), an additional Lorentzian line broadening  $\Delta_2$  can be calculated in the way it was derived by Abragam for scalar relaxation of the second kind:<sup>49</sup>

$$\Delta_2 = \frac{4}{5\pi} \frac{(\gamma_I \gamma_S \hbar)^2}{r^6} P_2^2(\cos \theta_{\text{DQ}}) \tau \quad (11)$$

A remarkable feature of eq 11 is that  $\Delta_2$  does not depend on the quadrupolar coupling constant and resembles closely the dipolar line broadening. Besides the factor  $P_2^2(\cos \theta_{\text{DQ}})$ ,  $\Delta_2$  equals 1.5 times the heteronuclear dipolar broadening in the slow motion limit as calculated from the formula for the dipolar  $T_2$  of two different spins.<sup>50</sup>

For the proton-deuteron system, at a distance of 2 Å,  $\theta_{\text{DQ}} = 0$ , and  $\tau = 8$  (16) ns, a proton line broadening of 0.4 Hz (0.9 Hz) is calculated according to eq 11. For a proton in an otherwise uniformly deuterated macromolecule, all the different asymmetric splittings will superimpose. However, we see from the  $r^{-6}$  dependence in eq 11 that only next neighbors will contribute significantly to the line broadening.

The asymmetric splitting should also be noticeable for amide  $^{15}\text{N}$  nuclei attached to amide deuterons. In this case, for an amide deuteron bond length of 1.02 Å, in the slow motion limit, and at a 600 MHz proton Larmor frequency ( $\theta_{\text{DQ}} = 0$ ,  $\eta = 0$ ), the asymmetric splitting  $\Delta$  would be 2.9 Hz (eq 9).

It is interesting to observe that there is also some effect for a  $^1\text{H}$ - $^{14}\text{N}$  system in liquid solution. Recent data<sup>29</sup> indicate that the quadrupolar coupling constant for amide  $^{14}\text{N}$  has a value of  $-3.2$  MHz, with  $\eta = 0.22$ , the largest component of the nitrogen electric field tensor  $eq_{zz}$  is perpendicular to the amide plane, and the component  $eq_{xx}$  makes an angle of  $19^\circ$  with the amide bond vector. In the slow motion limit with those values, the asymmetric

(49) Reference 30, p 504.

(50) Reference 30, p 296.

splitting  $\Delta$  according to eq 9 is 272 Hz (the assumption of cylindrical symmetry introduces a maximal error of 20%). Due to the large quadrupolar coupling constant, the  $^{14}\text{N}$  spin flip rate is however much faster than the  $^2\text{H}$  spin flip rate. From eq 11, an additional proton line broadening of 1.3 Hz (2.6 Hz) is calculated for a rotational correlation time of 8 ns (16 ns). This broadening is 9–10 times larger than the contribution of scalar relaxation of the second kind assuming a  $J_{\text{H}^{14}\text{N}}$  coupling of 66 Hz.

**Acknowledgment.** We thank James Omichinski and Joe Barchi for the distillation of the glycerol, Jim Ferretti for generously letting us use his 360 MHz spectrometer, Attila Szabo and Dennis Torchia for many useful theoretical suggestions, Andy Wang for critical comments on the paper, and Rolf Tschudin for spectrometer hardware modifications. This work was supported by the Intramural AIDS Targeted Anti-Viral Program of the Office of the Director of the National Institutes of Health.

**Note Added in Proof.** By a stimulating discussion with Prof. R. R. Vold we became aware of the work of Voigt and Jacobsen<sup>51</sup> who give evidence and a detailed theory for dipolar/quadrupolar interference effects of spin-1/2-spin-1 systems in nematic phases.

## Appendix

Matrix elements in the three-dimensional subspace of eq 7 of the products  $\underline{D}X_m^\alpha \cdot \underline{D}X_m^{\alpha\dagger}$  (pure dipolar relaxation)

$$\langle \langle i | \underline{D}X_0^1 \cdot \underline{D}X_0^{1\dagger} | j \rangle \rangle = \begin{pmatrix} 2/3 & 0 & 0 \\ 0 & 0 & 0 \\ 0 & 0 & 2/3 \end{pmatrix} \quad (\text{A1})$$

(51) Voigt, J.; Jacobsen, J. P. *J. Chem. Phys.* **1983**, *78*, 1693–1702.

$$\langle \langle i | \underline{D}X_0^2 \cdot \underline{D}X_0^{2\dagger} | j \rangle \rangle = \begin{pmatrix} 1/12 & 0 & 0 \\ 0 & 1/6 & 0 \\ 0 & 0 & 1/12 \end{pmatrix}$$

$$\langle \langle i | \underline{D}X_1^1 \cdot \underline{D}X_1^{1\dagger} | j \rangle \rangle = \langle \langle i | \underline{D}X_{-1}^1 \cdot \underline{D}X_{-1}^{1\dagger} | j \rangle \rangle = \begin{pmatrix} 1/8 & 1/8 & 0 \\ 1/8 & 1/4 & 1/8 \\ 0 & 1/8 & 1/8 \end{pmatrix}$$

$$\langle \langle i | \underline{D}X_1^2 \cdot \underline{D}X_1^{2\dagger} | j \rangle \rangle = \begin{pmatrix} 1/2 & 0 & 0 \\ 0 & 0 & 0 \\ 0 & 0 & 1/2 \end{pmatrix}$$

$$\langle \langle i | \underline{D}X_2^1 \cdot \underline{D}X_2^{1\dagger} | j \rangle \rangle = \begin{pmatrix} 1/2 & 0 & 0 \\ 0 & 1 & 0 \\ 0 & 0 & 1/2 \end{pmatrix}$$

$$\langle \langle i | \underline{D}X_0^3 \cdot \underline{D}X_0^{3\dagger} | j \rangle \rangle = \langle \langle i | \underline{D}X_{-1}^2 \cdot \underline{D}X_{-1}^{2\dagger} | j \rangle \rangle = \langle \langle i | \underline{D}X_{-2}^1 \cdot \underline{D}X_{-2}^{1\dagger} | j \rangle \rangle = 0$$

and of the products  $\underline{Q}X_m^\alpha \cdot \underline{Q}X_m^{\alpha\dagger}$  (pure quadrupolar relaxation)

$$\langle \langle i | \underline{Q}X_0^1 \cdot \underline{Q}X_0^{1\dagger} | j \rangle \rangle = 0 \quad (\text{A2})$$

$$\langle \langle i | \underline{Q}X_1^1 \cdot \underline{Q}X_1^{1\dagger} | j \rangle \rangle = \langle \langle i | \underline{Q}X_{-1}^1 \cdot \underline{Q}X_{-1}^{1\dagger} | j \rangle \rangle = \begin{pmatrix} 3 & -3 & 0 \\ -3 & 6 & -3 \\ 0 & -3 & 3 \end{pmatrix}$$

$$\langle \langle i | \underline{Q}X_2^1 \cdot \underline{Q}X_2^{1\dagger} | j \rangle \rangle = \langle \langle i | \underline{Q}X_{-2}^1 \cdot \underline{Q}X_{-2}^{1\dagger} | j \rangle \rangle = \begin{pmatrix} 6 & 0 & -6 \\ 0 & 0 & 0 \\ -6 & 0 & 6 \end{pmatrix}$$